FERMILAB-CONF-23-0875-AD
14th International Particle Accelerator Conference,Venice, Italy JACoW Publishing
ISBN: 978-3-95450-231-8 ISSN: 2673-5490 doi: 10.18429/JACoW-IPAC2023-THPL095

MEASUREMENT OF BEAM ENERGY IN THE FERMILAB'S LINAC TAKEN AT THE TRANSFER LINE*

M.W. Mwaniki[1†],K.Seiya and R.V. Sharankova, Fermi National Laboratory, Batavia, IL 60510, USA
[1]also at Illinois Institute of Technology, Chicago,IL 60616, USA

Abstract

Linac is the first machine in the accelerator chain at Fermilab where H^- ions are accelerated from 35 keV to 401.5 MeV and then injected into a synchronton known as Booster where they are stripped of their electrons to become protons. One of the tools used during tuning of the Linac extraction energy is two beam pickups known as Griffin Detectors. Our goal is to control the output energy using machine learning techniques to increase the reliability and quality of the beam delivered from Linac. The first step is to understand the data from the diagnostics to develop reliable and accurate energy measurement, and control methods before implementing machine learning techniques. Two methods of energy measurement were studied, and their results are compared. The first method was the time of flight measurement using Beam Position Monitors that provide beam phase measurement. The second method used the relation between beam transverse positions and dispersion values to calculate momentum variation. The results of these two measurement methods are found to be consistent.

INTRODUCTION

400 MeV Line

The Linac is the first machine in the accelerator chain at Fermilab. It accelerates H^- ions from 35 keV to 400 MeV that get injected into the Booster via the 400 MeV transfer line, which also offers lattice matching. [1]

The beginning of the transfer line is shown in Figure. 1. The first element is the chopper that deflects the beam vertically up into the field region of the Lambertson where the beam experiences a westward horizontal bend. The upward deflection is corrected by a small dipole, MV0 so that it is parallel to the enclosure floor. It then encounters a horizontal bend eastwards from a dipole, MH1. Once the beam has gone through Quad 4, it encounters a downward bend of about 12 degrees towards the Booster enclosure. [2]

The major diagnostics in the line include: Beam Loss Monitors (BLMs), Beam Position monitors (BPMs) that can measure both beam position and the longitudinal phase of the beam, and two beam velocity pickups (called Griffin Detectors). The latter are in-house strip-line detectors that also measure the time of arrival of the beam.

Efforts are underway to revisit diagnostics in the Linac to understand their signals and to ensure they are reliable [3]. This is beacuse, to fulfil our ultimate goal of developing ML-based algorithms for energy control [4], we require robust diagnostic data.

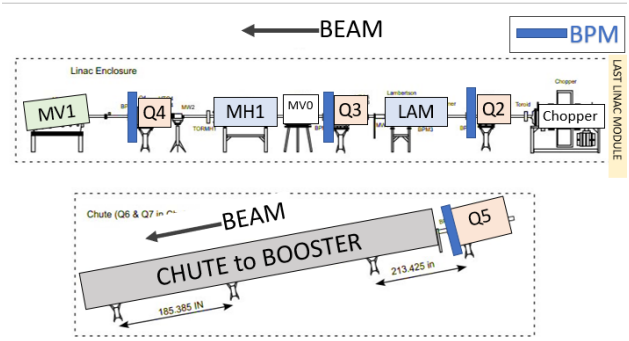

Figure 1: The beginning of the 400 MeV transfer line in the Linac enclosure to the wall of the chute. The 400 MeV line consists of quadrupoles, bend elements, and diagnostics.

Energy Measurement and Correction Methods

As the beam passes through an acceleration gap of an RF cavity at a phase Φ_{RF}, it receives an energy gain, ΔW:

$$\Delta W \propto V \cos \Phi_{RF} \tag{1}$$

Using this, output energy is controlled by adjusting the phase of the last RF cavity.

Linac output energy is measured via two methods: time-of-flight (TOF) method, and dispersion method. Those methods will be described in detail in the following sections.

TIME OF FLIGHT METHOD

Time of flight (TOF) is the time beam takes to travel between two pick-ups separated by a distance, L. Beam energy can be measured from the velocity estimated from TOF. There are four BPMs in the 400 MeV transfer line as shown in Figure 1. TOF is calculated from the difference in the phase of beam arrival between the second BPM and the n-th BPM. [5]

Analysis Using the TOF Method

1. An offset, $\Delta\phi_n$, is measured as the phase difference between the reference RF signal and BPM phase signal in the absence of beam, and subsequently subtracted from the BPM phase in the presence of the beam.

2. BPM data was collected during an RF phase scan of the last cavity in the range 45 to 100 degrees as shown in Figure 2.

* WORK SUPPORTED BY THE U.S. DEPARTMENT OF ENERGY, OFFICE OF SCIENCE, OFFICE OF HIGH ENERGY.
† mmwaniki@hawk.iit.edu

ISBN: 978-3-95450-231-8 ISSN: 2673-5490 doi: 10.18429/JACoW-IPAC2023-THPL095

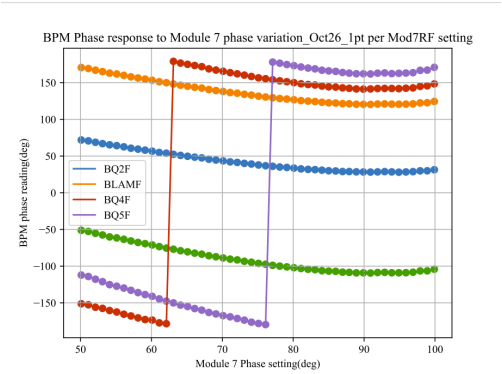

Figure 2: BPM phase response to last Linac RF cavity phase. Blue trace is the phase measured at the second BPM, Orange is the third, Green is the fourth, Red is the fifth, and Purple is the sixth. The discontinuities are from the phase signal range.

3. BPM output signal is in the range of ±180 degrees that cause discontinuities in the data. Therefore, 360 degrees need to be added to the negative values to make the signal continuous. The offset phase is subtracted from the continuous signal to synchronize the phase information between different BPMs.

4. The 2nd BPM in the line, BQ2F, is picked as the reference from which the beam phase is measured by taking the phase difference between each BPM,ϕ_n, and BQ2F,ϕ_2.
where: $\phi_n \equiv \tilde{\phi}_n - \Delta\phi_n$.

5. Estimated integer phase periods, $K_n \pm 1$, between BQ2F and the n-th BPM by estimating β at 401.5 MeV.

$$K_n = Quotient\ of\ \left(\frac{L_n - L_2}{c \cdot \beta_{401.5\ MeV}} \times f_{BPM}\right) \pm 1 \quad (2)$$

where, $L_n \equiv$ distance from the start to the n-th BPM and $f_{BPM} = 402MHz$.

6. The total measured phase, ϕ_{tot}, is then acquired using the calculated integer RF periods and the measured fractional phase as:

$$\phi_{tot} = (\phi_n - \phi_2) + 360 \cdot K_n \quad (3)$$

The total phase is converted to TOF as in Eq. 4

$$TOF_{measured} = \frac{\phi_{tot}}{360 \times f_{BPM}} \quad (4)$$

7. Beam energy calculated using Equation 5 is plotted in Figure 3.

$$E = E_0\left(\frac{c \cdot TOF_{measured}}{\sqrt{c^2 \cdot TOF^2_{measured} - (L_n - L_2)^2}} - 1\right) \quad (5)$$

where E_0 is the rest energy of H^-.

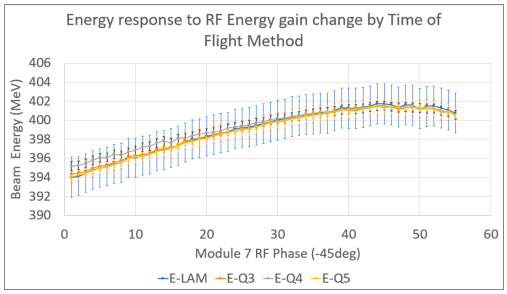

Figure 3: Beam energy from TOF as a function of last linac RF cavity phase. Error bars from error analysis.

8. The systematic errors from the TOF method included in the plot on Figure. 3 arise from:

   (a) BPM phase resolution as measured in [7]

   (b) Length accuracy from design (1993), alignment data (1993), and tape measurement (2022) is 0.01 m or less. This gives a dE/E of 0.5% or less.

DISPERSION METHOD

During acceleration, off-momentum particles undergo betatron oscillations with different trajectories whose displacement from the ideal trajectory will be described by a momentum dispersion function.

As high momentum beam centroid travels through bending elements, it receives less bending while low momentum beam centroid receives more bending. A transverse deviation from the ideal trajectory as recorded by the BPMs can be related to momentum variation as:

$$\Delta x = \mathbb{D}(s)\frac{\Delta p}{p} \quad (6)$$

where, $\mathbb{D}$ is the dispersion value, $\frac{\Delta p}{p}$ is the momentum deviation from the ideal momentum and Δx is the transverse deviation from the ideal trajectory.

The 400 MeV lattice was simulated using MADX [8] code to estimate a beam trajectory and dispersion function at each BPM location.

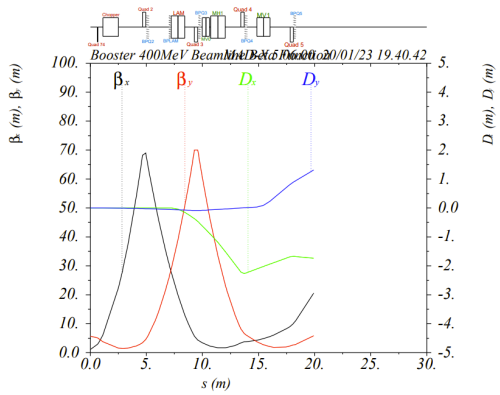

Figure 4: MADX output graphic file

ISBN: 978-3-95450-231-8 ISSN: 2673-5490 doi: 10.18429/JACoW-IPAC2023-THPL095

The data used in this method of measurement is collected as described in Section Time of Flight method.

Analysis for the Dispersion Method

1. There is 2 horizontal and 1 vertical bending magnet between the 2nd BPM and 5th BPM that create dispersion. The dispersion at BPM locations, as calculated with MADX, is listed in Table. 1.

Table 1: Dispersion Values From the MADX Model in the High Dispersion Regions

Name	S	Dx	Dy
L400START	0 m	0 m	0 m
BPH/VQ3	9.731 70 m	−0.523 98 m	−0.083 96 m
BPH/VQ4	13.8732 m	−2.245 05 m	0.007 59 m
BPH/VQ5	18.2196 m	−1.673 66 m	0.984 73 m

2. Beam transverse positions as a function of the last RF cavity phase were collected as described in (Section. Time of Flight) and plotted in Figure 5

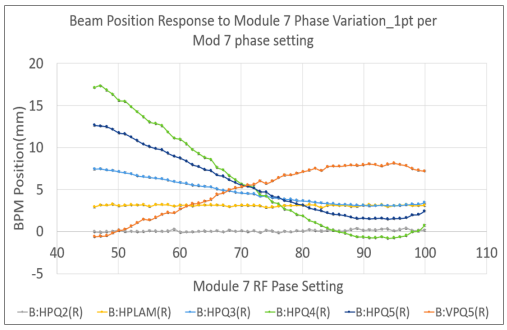

Figure 5: Beam transverse positions vs last RF cavity phase.

3. The reference transverse BPM position is defined as the BPM reading at Linac last cavity operational RF phase setting. This is because it is set at a value that ensures favorable beam energy at Booster injection. The position differences from the reference transverse position Δx(horizontal) or Δy(vertical) are calculated.

4. The momentum deviation, $\frac{\Delta p}{p}$, is then calculated using the Δx and the dispersion values from Table. 1. The results are shown in Figure. 6

5. There are 2 sources of systematic error in Figure 6. One is BPM position resolution of 0.1 (mm) [7]. The second is uncertainty in dispersion values calculated in MADX. This was estimated by varying the current in the bending magnets which affects the trajectory length.

DISCUSSION

In the current operational setup, the Griffin detectors only measure relative fluctuations in energy [6]. Additionally, it uses an analogue phase mixer circuit which has been found

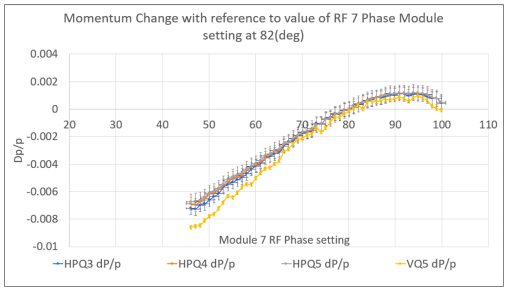

Figure 6: dp/p calculated from dispersion plotted against the last Linac RF cavity phase. Error bars from error analysis.

to show non-linear effects. [3] Thus the development of the above methods for accurate energy measurements is crucial towards the goal of energy control with machine learning techniques. Energy as measured by the TOF method was translated to dp/p. From the collected RF cavity phase scan dataset, it is assumed the data point at the operational RF Phase corresponds to the design energy of 401.5 MeV. Measurements of the two methods are compared in Figure 7. The two methods give largely consistent results within the systematic errors of the dispersion method. Note that TOF errors are not shown here. the

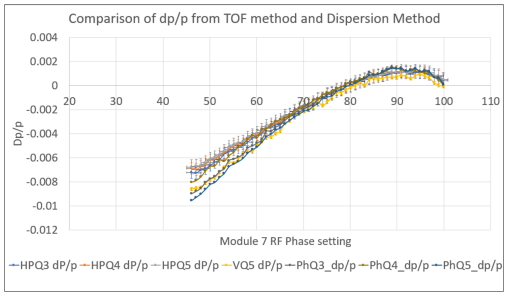

Figure 7: dp/p calculated from both methods plotted against the Last Linac Cavity RF phase. Error bars are from the Dispersion method only.

CONCLUSION

The absolute beam energy was measured in the 400 MeV line where there are no accelerating elements, using the time-of-flight and the dispersion methods.
The two methods agree within systematic errors.
The next step is to develop an ML-based control mechanism for Linac Output energy regulation.

ACKNOWLEDGEMENTS

This Work is supported by Fermilab Research Alliance, LLC under Contract No. DE-AC02-07CH11359 with the United States Department of Energy.

REFERENCES

[1] Johnstone, C., "400MeV General Document", for FNAL Booster Dept, March 1, 1993

ISBN: 978-3-95450-231-8 ISSN: 2673-5490 doi: 10.18429/JACoW-IPAC2023-THPL095

[2] Patterson D., Gattuso C., Worthel B., Sullivan T., McCrory E., Schmidt C., Wahl L., and Florian R. "Linac Rookie Book", in Fermi National Laboratory https://operations.fnal.gov/rookie_books/LINAC_RB_v2_3.pdf, April 2004

[3] R.V. Sharankova, M.W. Mwaniki, K. Seiya, and M.E. Wesley, "Diagnostics for LINAC Optimization with Machine Learning", in *Proc. 5th Int. Particle Accel. Conf. (NAPAC'22)*, Albuquerque, NM, USA, Aug. 2022, pp. 139–142.

[4] R.V. Sharankova, M.W. Mwaniki, K. Seiya, and M.E. Wesley, "Time-drift aware RF optimization with machine learning techniques", presented at *14th Int. Particle Accel. Conf.(IPAC'23)*, Venice, Italy, May. 2023

[5] Wong, C.Y.J. and Shishlo, A., "Time-of-Flight Calculations with Multiple Beam Phase Monitors: Calibration, Jitter Analysis, and Energy Measurement", in *Oakridge Lab*, April 2022

[6] Drennan, C., "Linac Beam Velocity/Energy Measurement", https://beamdocs.fnal.gov/cgi-bin/sso/ShowDocument?docid=3889, 24 Jul 2012.

[7] E. McCrory, N. Eddy, F. G. Garcia, S. Hansen, T. Kiper and M. Sliczniak, "BPM Electronics Upgrade for the Fermilab H- Linac Based Upon Custom Downconverter Electronics," FERMILAB-CONF-13-447-AD.

[8] L. Deniau, H. Grote, G. Roy, F. Schmidt, "The MAD-X Program (Methodical Accelerator Design)," https://mad.web.cern.ch/mad/, Feb 25,2022.